

# Effects of temperature fluctuation on highly dispersive photonic crystal fibers

Yongqiang Jiang, Xiaonan Chen, and Brie Howley

Microelectronic Research Center, Department of Electrical and Computer Engineering,  
The University of Texas at Austin, Austin, Texas 78758

Maggie Y. Chen

Omega Optics, Austin, Texas 78758

Ray T. Chen<sup>a)</sup>

Microelectronic Research Center, Department of Electrical and Computer Engineering,  
The University of Texas at Austin, Austin, Texas 78758

(Received 7 April 2005; accepted 7 November 2005; published online 4 January 2006)

Chromatic dispersion of highly dispersive photonic crystal fibers (PCFs) is theoretically simulated and experimentally measured as a function of temperature. We have theoretically confirmed that PCFs designed at highly dispersive region show stronger temperature dependence than conventional telecommunication fibers and dispersion compensation fibers due to phase matching wavelength shift and large dispersion slope. For a fabricated highly dispersive PCF, the variation of the dispersion is measured to be around  $+0.28\% / ^\circ\text{C}$  from 21 to  $80^\circ\text{C}$ , and around  $+0.21\% / ^\circ\text{C}$  from 21 to  $50^\circ\text{C}$  at an optical wavelength around 1550 nm. © 2006 American Institute of Physics. [DOI: 10.1063/1.2162684]

Photonic crystal fibers (PCFs) have generated a lot of interest due to their unusual and attractive properties such as high chromatic dispersion, endless single mode, large numerical aperture, and enhanced nonlinearity.<sup>1–6</sup> PCFs are usually made of silica or polymer material with a regular hexagonal array of sub-micrometer-sized air holes running along the fiber axis as a cladding. A defect, usually one or multiple missing holes, acts as core. Conventional single-mode fibers, which are based on weakly guiding structures with doped silica, can be tailored to slightly increase the dispersion by increasing the refractive index difference between the core and cladding.<sup>6</sup> However, the dispersion cannot be changed significantly because of the small index variation across the transverse cross section of the fiber from doping. This shortcoming can be overcome by the employment of PCFs, which have more freedom to enhance the dispersion. Owing to their high dispersion, PCFs can be used as dispersion compensation fibers to minimize the penalty by dispersion of large bandwidth optical networks.<sup>5,6</sup> We recently demonstrated a dispersion enhanced wavelength tunable true-time delay technique for an X-band phased array antenna using highly dispersive PCFs.<sup>7,8</sup> In all of these systems, thermal sensitivity is an important factor for practical applications. Schneider *et al.*<sup>9</sup> and Kato *et al.*<sup>10</sup> demonstrated the temperature dependence of the chromatic dispersion of conventional fibers including telecommunication fibers and dispersion compensation fibers. However, to our knowledge there is no report about the temperature dependence of the chromatic dispersion of highly dispersive PCFs. In this letter, the temperature dependence of the chromatic dispersion of the highly dispersive PCFs is analyzed, simulated, measured, and the results are discussed.

We simulated several highly dispersive PCFs. We use a dual-core PCF design to achieve high dispersion. An index

profile of the cross section of the PCF is shown in Fig. 1. In our design, we use different doping concentrations  $n_1$ ,  $n_2$ , period  $\Lambda$ , and hole diameters  $d_0$ ,  $d_1$ ,  $d_2$ , and  $d$ , to enhance the dispersion. Here,  $d_0$  and  $d_2$  are the diameters of the inner and outer doped silica rods, respectively, and  $d_1$  and  $d$  are the diameters of the air holes. By tuning these parameters, we can obtain a large dispersion parameter  $D$  value that we desire. The inner core is a doped silica rod, and the outer core is 12 concentric doped silica rods. Both cores are doped to have larger refractive index than pure silica, but the refractive index of the inner core is greater than that of the outer core. The design parameters are  $\Lambda=3.50\ \mu\text{m}$ ,  $d=0.86\ \mu\text{m}$ ,  $d_0=1.72\ \mu\text{m}$ ,  $d_1=1.45\ \mu\text{m}$ ,  $d_2=1.08\ \mu\text{m}$ ,  $\Delta n_1/n=1.9\%$ , and  $\Delta n_2/n=1.2\%$ .<sup>7,8</sup> This dual-core PCF can support two supermodes, which are analogous to the two supermodes of a directional coupler.<sup>9,11</sup> These modes are nearly phase

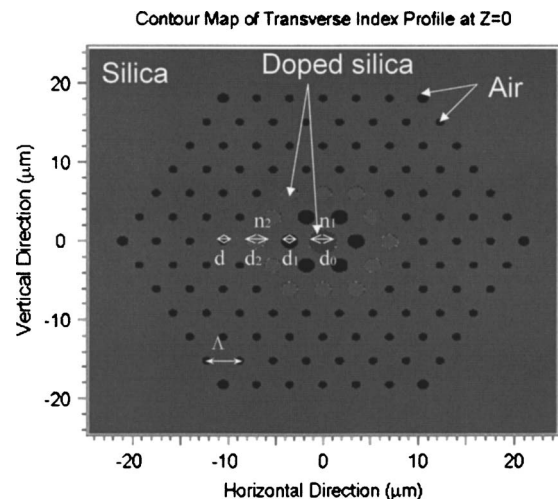


FIG. 1. Index profile of the highly dispersive PCF (see Ref. 8) with  $\Lambda=3.50\ \mu\text{m}$ ,  $d=0.86\ \mu\text{m}$ ,  $d_0=1.72\ \mu\text{m}$ ,  $d_1=1.45\ \mu\text{m}$ ,  $d_2=1.08\ \mu\text{m}$ ,  $\Delta n_1/n=1.9\%$ , and  $\Delta n_2/n=1.2\%$ .

<sup>a)</sup> Author to whom correspondence should be addressed; electronic mail: chen@ece.utexas.edu

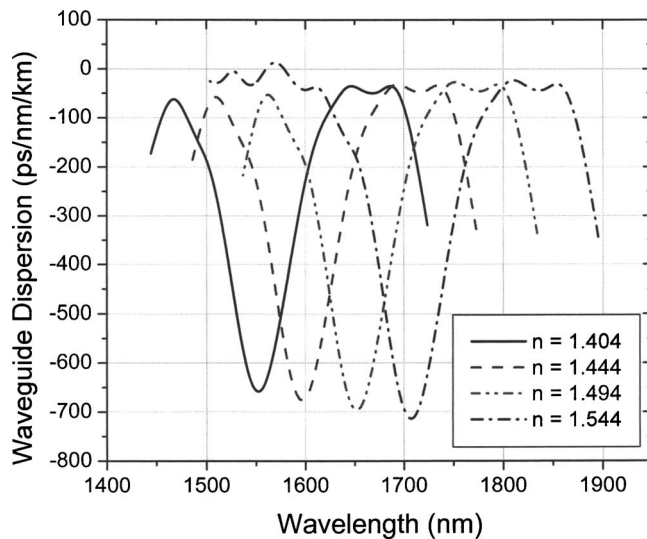


FIG. 2. Waveguide dispersion vs wavelength at different material refractive index  $n$  for the highly dispersive PCF. Redshift of  $\lambda_p$  is clearly seen as  $n$  increases.

matched at the wavelength  $\lambda_p$ . Close to the phase matching wavelength, the mode index of the PCF changes rapidly due to strong coupling between the two individual modes of the inner and outer cores. Due to strong refractive index asymmetry between the two cores, there is a rapid change of the slope of the wavelength variation of the fundamental mode index. This leads to large dispersion around the phase matching wavelength  $\lambda_p$ . The periodic air hole structure of PCFs helps not only to guide the mode, but also to increase the dispersion value. However, due to the resonant nature of the coupling in PCFs, any small change (for example, temperature) will lead to the shift of  $\lambda_p$  resulting in a dramatic change of dispersion parameter  $D$  due to the large dispersion slope  $dD/d\lambda$ .

As we know, the dispersion parameter  $D$  of a single-mode fiber is composed of material dispersion  $D_m$  and waveguide dispersion  $D_w$ , with the relation of  $D = D_m + D_w$ .<sup>3,6</sup>  $D_m$  only depends on material property and does not change with fiber design. For highly dispersive PCFs,  $D_w$  is usually at least one order greater than  $D_m$ . The thermo coefficient of the material refractive index of fused silica is  $+1.2 \times 10^{-5}/^\circ\text{C}$  at an optical wavelength around 1550 nm.<sup>12</sup> This means the material refractive index of fused silica increases 0.0012 if the temperature increases 100 °C. However, the shift of  $\lambda_p$  is only within 1 nm. In order to accurately measure the temperature dependence of the waveguide dispersion of PCFs, we need a large  $\lambda_p$  shift. Thus we choose a large index change in the simulation. In our simulation, we use the full vectorial plane wave expansion (PWE) method which is fast and accurate compared to other methods.<sup>7,8</sup> Since our PCF design is not a perfect crystal without defects, we need to use a supercell having a size of  $N \times N$  instead of natural unit cell to implement the periodic boundary conditions.<sup>7,8</sup> We use commercial software RSOFT BANDSOLVE to run the PWE simulation on PCFs. The grid size is 20 nm. The unit cell is  $8 \times 8$ . Figure 1(b) shows the simulated dispersion versus wavelength curve of PCF #1 at various material refractive indexes of  $n=1.404$ , 1.444, 1.494, and 1.544, respectively. From Fig. 1(b) we can easily see the redshift of  $\lambda_p$  as we increase the material index. We can also see that the shift of  $\lambda_p$  is proportional to material refractive index change. The  $\lambda_p$

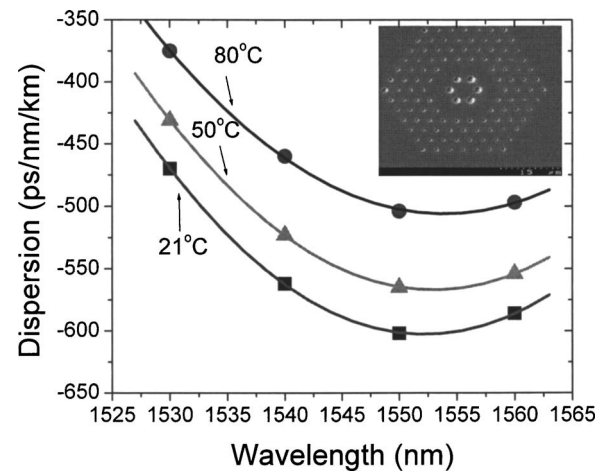


FIG. 3. Measured chromatic dispersion vs wavelength at different temperatures for highly dispersive photonic crystal fiber. Inset is a scanning electron micrograph image of the fabricated highly dispersive PCFs.

shifts +50 nm when the material refractive index increases 0.05. The  $\lambda_p$  shifts proportional to temperature change and it shifts to longer wavelength when temperature increases. For example, suppose temperature increases 100 °C, the refractive index of fused silica will increase 0.0012, which corresponds to a redshift of 1 nm for  $\lambda_p$ . However, the dispersion slope  $dD/d\lambda$  of highly dispersive PCF is usually at least one or two orders larger than conventional telecom fibers and dispersion compensation fibers.<sup>9,10</sup> The dispersion change  $dD/dT$  is proportional to dispersion slope  $dD/d\lambda$ , and phase matching wavelength shift  $d\lambda_p/dT$ . This explains why high dispersive PCFs have a larger temperature dependence of dispersion than conventional telecom fiber<sup>10</sup> and dispersion compensation fiber.<sup>9,10</sup>

Photonic crystals provide a much larger range of group velocities that are intrinsically highly sensitive to refractive index perturbation.<sup>13</sup> Therefore, any PCF designed at the highly dispersive region will have larger environmental sensitivity; for example, temperature sensitivity. We have simulated PCFs with various parameters:  $d$ ,  $d_0$ ,  $d_1$ ,  $d_2$ ,  $d_3$ ,  $n_1$ ,  $n_2$ , and  $\Lambda$  (Fig. 1). Dispersion enhancements of one to two orders of magnitude are confirmed.

The highly dispersive PCF is fabricated using the stack-and-draw technique, where silica glass capillaries are stacked in a desired lattice array, fused together, and then drawn down to PCFs.<sup>3,4</sup> A scanning electron micrograph image of the cross section is shown in the inset of Fig. 3. In order to measure the chromatic dispersion of the fabricated highly dispersive PCFs, we measured the time delay between optical wavelengths of  $(\lambda_o + 0.5 \text{ nm})$  and  $(\lambda_o - 0.5 \text{ nm})$  using the setup described in Ref. 14. To obtain the time delay, we measured the rf phase as a function of microwave frequency ranging from 8 to 12 GHz. The time delay can be derived from the slope of the each curve. The fiber chromatic dispersion is defined as  $\Delta T/(\Delta\lambda \cdot L)$ , which can be obtained from the time delay divided by the fiber length and optical laser wavelength difference, which is 1 nm in this case. A copper pipe was lined with a heating blanket that was connected to a proportional integral derivative (PID) temperature controller.<sup>14</sup> A thermocouple was externally attached to the copper pipe with thermally conductive epoxy. The thermocouple was connected to the PID controller to form a feedback loop. The sample fibers were wrapped around the out-

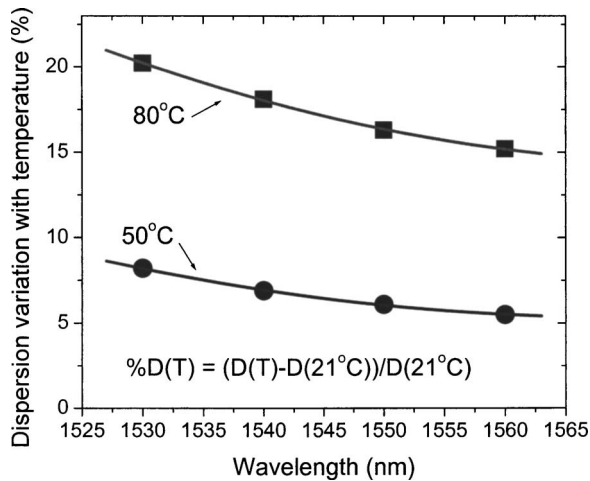


FIG. 4. Dispersion shift versus wavelengths at 50 and 80 °C.

side of the copper pipe and dispersion measurements were made at the temperatures of 21, 50, and 80 °C. A waiting period of 1 h or more was allowed between temperature cycles to ensure the thermal equilibrium of the fiber sample. The measurement results are shown in Fig. 3. Changes of the dispersion with relation to the temperature at a given wavelength can be calculated by

$$%D(\lambda, T) = [D(\lambda, T) - D(\lambda, 21 \text{ } ^\circ\text{C})] / D(\lambda, 21 \text{ } ^\circ\text{C}). \quad (1)$$

Typical shifts of the dispersion with a change in temperature are shown in Fig. 4. The dispersion shift is approximately +0.28% / °C from 21 to 80 °C, and approximately +0.21% / °C from 21 to 50 °C. This property may be useful for certain thermal sensors if the PCFs are carefully designed. For those applications trying to avoid this thermal sensitivity of dispersion, one can use a temperature controller. Another possible solution is to use another high dispersion fiber with an opposite temperature sensitivity in order to

compensate for the change of dispersion due to the temperature change.

In summary, chromatic dispersion of highly dispersive photonic crystal fiber is theoretically simulated and experimentally measured as a function of temperature. Highly dispersive photonic crystal fibers show greater temperature dependence than conventional telecom fibers and dispersion compensation fibers due mainly to phase matching wavelength shift and large dispersion slope. For a fabricated highly dispersive PCF, the variation of the dispersion is measured to be around +0.28% / °C from 21 to 80 °C, and around +0.21% / °C from 21 to 50 °C at optical wavelength around 1550 nm.

This research is sponsored by Defense Advanced Research Projects Agency.

- <sup>1</sup>J. C. Knight, T. A. Birks, P. St. J. Russell, and D. M. Atkin, *Opt. Lett.* **21**, 1547 (1996); **22**, 484(E) (1997).
- <sup>2</sup>J. Broeng, D. Mogilevtsev, S. E. Barkou, and A. Bjarklev, *Opt. Fiber Technol.* **5**, 305 (1999).
- <sup>3</sup>A. Bjarklev, J. Broeng, and A. S. Bjarklev, *Photonic Crystal Fibers* (Kluwer Academic, 2003).
- <sup>4</sup>P. S. J. Russell, *Science* **299**, 358 (2003).
- <sup>5</sup>T. A. Birks, D. Mogilevtsev, J. C. Knight, and P. St. J. Russell, *IEEE Photonics Technol. Lett.* **11**, 674 (1999).
- <sup>6</sup>L. P. Shen, W. P. Huang, G. X. Chen, and S. S. Jian, *IEEE Photonics Technol. Lett.* **15**, 540 (2003).
- <sup>7</sup>Y. Jiang, B. Howley, Z. Shi, Q. Zhou, R. T. Chen, M. Y. Chen, G. Brost, and C. Lee, *IEEE Photonics Technol. Lett.* **17**, 187 (2005).
- <sup>8</sup>Y. Jiang, Z. Shi, B. Howley, X. Chen, M. Y. Chen, and R. T. Chen (in press).
- <sup>9</sup>V. M. Schneider, *Electron. Lett.* **37**, 1069 (2001).
- <sup>10</sup>T. K. Kato, Y. Koyano, and M. Nishimura, *Opt. Lett.* **25**, 1156 (2000).
- <sup>11</sup>K. Thyagarajan, R. K. Varshney, and P. Palai, *IEEE Photonics Technol. Lett.* **8**, 1510 (1996).
- <sup>12</sup>T. Toyoda and M. Yabe, *J. Phys. D* **16**, L97 (1983).
- <sup>13</sup>M. Soljacic, S. G. Johnson, S. Fan, M. Ibanescu, E. Ippen, and J. D. Joannopoulos, *J. Opt. Soc. Am. B* **19**, 2052 (2002).
- <sup>14</sup>B. Howley, Z. Shi, Y. Jiang, and R. T. Chen, *Opt. Laser Technol.* **37**, 29 (2004).